Chapter 24

Deterministic diffusion

This is a bizzare and discordant situation.
—M.V. Berry

(R. Artuso and P. Cvitanović)

THE ADVANCES in the theory of dynamical systems have brought a new life to Boltzmann's mechanical formulation of statistical mechanics. Sinai, Ruelle and Bowen (SRB) have generalized Boltzmann's notion of ergodicity for a constant energy surface for a Hamiltonian system in equilibrium to dissipative systems in nonequilibrium stationary states. In this more general setting the attractor plays the role of a constant energy surface, and the SRB measure of sect. 19.1 is a generalization of the Liouville measure. Such measures are purely microscopic and indifferent to whether the system is at equilibrium, close to equilibrium or far from it. "Far for equilibrium" in this context refers to systems with large deviations from Maxwell's equilibrium velocity distribution. Furthermore, the theory of dynamical systems has yielded new sets of microscopic dynamics formulas for macroscopic observables such as diffusion constants and the pressure, to which we turn now.

We shall apply cycle expansions to the analysis of *transport* properties of chaotic systems.

The resulting formulas are exact; no probabilistic assumptions are made, and the all correlations are taken into account by the inclusion of cycles of all periods. The infinite extent systems for which the periodic orbit theory yields formulas for diffusion and other transport coefficients are spatially periodic, the global state space being tiled with copies of a elementary cell. The motivation are physical problems such as beam defocusing in particle accelerators or chaotic behavior of passive tracers in 2-dimensional rotating flows, problems which can be described as deterministic diffusion in periodic arrays.

In sect. 24.1 we derive the formulas for diffusion coefficients in a simple physical setting, the 2-dimensional periodic Lorentz gas. This system, however, is not

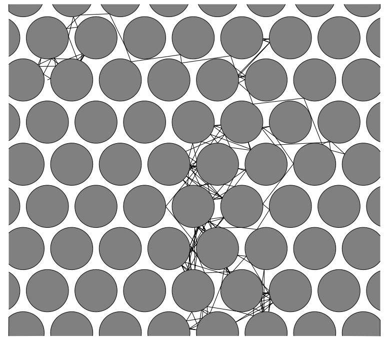

Figure 24.1: Deterministic diffusion in a finite horizon periodic Lorentz gas. (T. Zhang)

the best one to illustrate the theory, due to its complicated symbolic dynamics. Therefore we apply the theory first to diffusion induced by a 1-dimensional maps in sect. 24.2.

24.1 Diffusion in periodic arrays

Chaos happens - let's make a better use of it.
— Edward Tenner

The 2-dimensional *Lorentz gas* is an infinite scatterer array in which diffusion of a light molecule in a gas of heavy scatterers is modeled by the motion of a point particle in a plane bouncing off an array of reflecting disks. The Lorentz gas is called "gas" as one can equivalently think of it as consisting of any number of pointlike fast "light molecules" interacting only with the stationary "heavy molecules" and not among themselves. As the scatterer array is built up from only defocusing concave surfaces, it is a pure hyperbolic system, and one of the simplest nontrivial dynamical systems that exhibits deterministic diffusion, figure 24.1. We shall now show that the *periodic* Lorentz gas is amenable to a purely deterministic treatment. In this class of open dynamical systems quantities characterizing global dynamics, such as the Lyapunov exponent, pressure and diffusion constant, can be computed from the dynamics restricted to the elementary cell. The method applies to any hyperbolic dynamical system that is a periodic tiling $\hat{\mathcal{M}} = \bigcup_{\hat{n}\in T} \mathcal{M}_{\hat{n}}$ of the dynamical state space $\hat{\mathcal{M}}$ by *translates* $\mathcal{M}_{\hat{n}}$ of an *elementary cell* $\mathcal{M}$, with T the abelian group of lattice translations (see figure 24.2). If the scattering array has further discrete rotational and reflection symmetries (G/T is a point group), each elementary cell may be built from a *fundamental domain* $\widetilde{\mathcal{M}}$ by the action of a discrete (not necessarily abelian) group G. The symbol $\hat{\mathcal{M}}$ refers here to the full state space, i.e., both the spatial coordinates and the momenta. The spatial component of $\hat{\mathcal{M}}$ is the complement of the disks in the *whole* space.

We shall now relate the dynamics in $\mathcal{M}$ to diffusive properties of the Lorentz gas in $\hat{\mathcal{M}}$.

These concepts are best illustrated by a specific example, a Lorentz gas based on the hexagonal lattice Sinai billiard of figure 24.3.

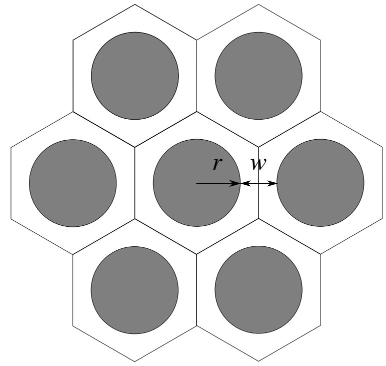

Figure 24.2: An elementary cell and its six nearest neighbor translations. The ratio (24.1) of the distance between the nearest pair disks and the disk radius determines the dynamical properties in the system: the horizon is finite for $w/r <= 0.3094\cdots$, and infinite beyond that. (T. Zhang)

We distinguish two types of diffusive behavior; the *infinite horizon* case, which allows for infinite length flights, and the *finite horizon* case, where any free particle trajectory must hit a disk in finite time. Consider figure 24.2, with w the distance between the nearest pair disks, and r the disk radius (here set to $r = 1$). The ratio w/r is the only parametar of the problem, the parameter that determines the dynamical properties in the system: the horizon is finite for

$$\frac{w}{r} < \frac{4}{\sqrt{3}} - 2 = 0.3094\cdots , \tag{24.1}$$

and infinite beyond that. In this chapter we shall restrict our consideration to the finite horizon case, with disks sufficiently large so that no infinite length free flight is possible. In this case the diffusion is normal, with $\hat{x}(t)^2$ growing like t. We shall discuss the anomalous diffusion case in sect. 24.3.

As we will work with three kinds of state spaces, good manners require that we repeat what tildes, nothings and hats atop symbols signify:

$$\begin{array}{ll} \tilde{} & \text{fundamental domain, triangle in figure 24.3} \\ & \text{elementary cell, hexagon in figure 24.3} \\ \hat{} & \text{full state space, lattice in figure 24.3} \end{array} \tag{24.2}$$

It is convenient to define an evolution operator for each of the 3 cases of figure 24.3. $\hat{x}(t) = \hat{f}^t(\hat{x})$ denotes the point in the global space $\hat{\mathcal{M}}$ reached by the flow in time t. $x(t) = f^t(x_0)$ denotes the corresponding flow in the elementary cell; the two are related by

$$\hat{n}_t(x_0) = \hat{f}^t(x_0) - f^t(x_0) \in T , \tag{24.3}$$

the translation of the endpoint of the global path into the elementary cell $\mathcal{M}$. The quantity $\tilde{x}(t) = \tilde{f}^t(\tilde{x})$ denotes the flow in the fundamental domain $\widetilde{\mathcal{M}}$; $\tilde{f}^t(\tilde{x})$ is related to $f^t(\tilde{x})$ by a discrete symmetry $g \in G$ which maps $\tilde{x}(t) \in \widetilde{\mathcal{M}}$ to $x(t) \in \mathcal{M}$. chapter 25

Fix a vector $\beta \in \mathbb{R}^d$, where d is the dimension of the state space. We will compute the diffusive properties of the Lorentz gas from the leading eigenvalue of the evolution operator (20.10)

$$s(\beta) = \lim_{t\to\infty} \frac{1}{t} \log\langle e^{\beta\cdot(\hat{x}(t)-x)}\rangle_{\mathcal{M}} , \tag{24.4}$$

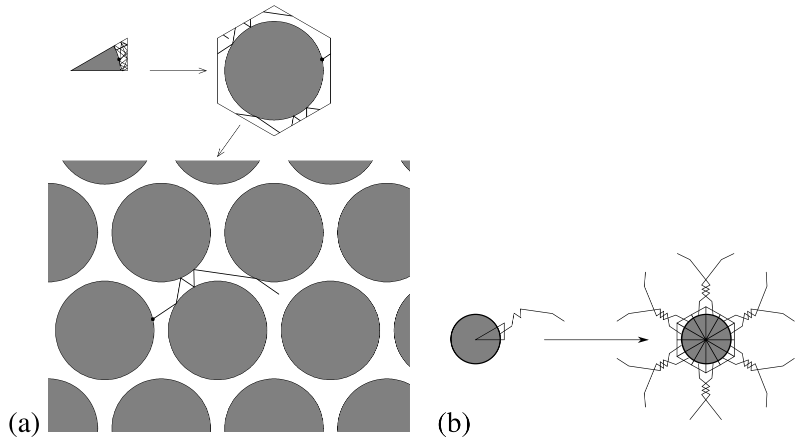

Figure 24.3: A periodic lattice of reflecting disks $\hat{\mathcal{M}}$ is tiled by copies of the fundamental domain $\widetilde{\mathcal{M}}$. (a) Motion in the fundamental domain $\widetilde{\mathcal{M}}$ (top left), the elementary cell $\mathcal{M}$ (top right), and the full state space $\hat{\mathcal{M}}$ (bottom). (b) The above trajectory unwrapped in the full space and its 11 copies obtained by applying the twelve D_6 point group actions to it. (From ref. [15]).

where the average is over all initial points in the elementary cell, $x \in \mathcal{M}$.

If all odd derivatives vanish by symmetry, there is no drift and the second derivatives

$$2dD_{ij} = \frac{\partial}{\partial\beta_i}\frac{\partial}{\partial\beta_j}s(\beta)\bigg|_{\beta=0} = \lim_{t\to\infty}\frac{1}{t}\langle(\hat{x}(t)-x)_i(\hat{x}(t)-x)_j\rangle_{\mathcal{M}}\,,$$

yield a diffusion matrix. This symmetric matrix can, in general, be anisotropic (i.e., have d distinct eigenvalues and eigenvectors). The spatial diffusion constant is then given by the Einstein relation (20.40)

$$D = \frac{1}{2d}\sum_i \frac{\partial^2}{\partial\beta_i^2}s(\beta)\bigg|_{\beta=0} = \lim_{t\to\infty}\frac{1}{2dt}\langle(\hat{q}(t)-q)^2\rangle_{\mathcal{M}}\ ,$$

where the i sum is restricted to the spatial components q_i of the state space vectors $x = (q, p)$, i.e., if the dynamics is Hamiltonian, the sum is over the d degrees of freedom.

We now turn to the connection between (24.4) and periodic orbits in the elementary cell. As the full $\hat{\mathcal{M}} \to \widetilde{\mathcal{M}}$ reduction is complicated by the non-abelian nature of G, we discuss only the abelian $\hat{\mathcal{M}} \to \mathcal{M}$ reduction. remark 24.5

24.1.1 Reduction from $\hat{\mathcal{M}}$ to $\mathcal{M}$

The key idea follows from inspection of the relation

$$\langle e^{\beta\cdot(\hat{x}(t)-x)}\rangle_{\mathcal{M}} = \frac{1}{|\mathcal{M}|}\int_{\substack{x\in\mathcal{M}\\ \hat{y}\in\hat{\mathcal{M}}}} dx d\hat{y}\, e^{\beta\cdot(\hat{y}-x)}\delta(\hat{y}-\hat{f}^t(x))\,.$$

$|\mathcal{M}| = \int_{\mathcal{M}} dx$ is the volume of the elementary cell $\mathcal{M}$. Due to translational symmetry, it suffices to start with a density of trajectories defined over a single elementary cell $\mathcal{M}$. As in sect. 20.3, we have used the identity $1 = \int_{\mathcal{M}} dy\, \delta(y - \hat{x}(t))$ to motivate the introduction of the evolution operator $\mathcal{L}^t(\hat{y}, x)$. There is a unique lattice translation $\hat{n}$ such that $\hat{y} = y - \hat{n}$, with the endpoint $y \in \mathcal{M}$ translated back to the elementary cell, and $f^t(x)$ given by (24.3). The difference is a translation by a constant lattice vector $\hat{n}$, and the Jacobian for changing integration from $d\hat{y}$ to dy equals unity. Therefore, and this is the main point, translation invariance can be used to reduce this average to the elementary cell:

$$\langle e^{\beta\cdot(\hat{x}(t)-x)}\rangle_{\mathcal{M}} = \frac{1}{|\mathcal{M}|}\int_{x,y\in\mathcal{M}} dxdy\, e^{\beta\cdot(\hat{f}^t(x)-x)}\delta(y - f^t(x)) \,. \tag{24.5}$$

As this is a translation, the Jacobian is $|\partial\hat{y}/\partial y| = 1$. In this way the global $\hat{f}^t(x)$ flow, infinite volume state space averages can be computed by following the flow $f^t(x_0)$ restricted to the compact, finite volume elementary cell $\mathcal{M}$. The equation (24.5) suggests that we study the evolution operator

$$\mathcal{L}^t(y, x) = e^{\beta\cdot(\hat{x}(t)-x)}\delta(y - f^t(x)) \,, \tag{24.6}$$

where $\hat{x}(t) = \hat{f}^t(x) \in \hat{\mathcal{M}}$ is the displacement in the full space, but $x, f^t(x), y \in \mathcal{M}$. It is straightforward to check that this operator satisfies the semigroup property (20.26),

$$\int_{\mathcal{M}} dz\, \mathcal{L}^{t_2}(y, z)\mathcal{L}^{t_1}(z, x) = \mathcal{L}^{t_2+t_1}(y, x) \ .$$

For $\beta = 0$, the operator (24.6) is the Perron-Frobenius operator (19.10), with the leading eigenvalue $e^{s_0} = 1$ because there is no escape from this system (see the flow conservation sum rule (23.17)).

The rest is old hat. The spectrum of $\mathcal{L}$ is evaluated by taking the trace section 21.2

$$\mathrm{tr}\,\mathcal{L}^t = \int_{\mathcal{M}} dx\, e^{\beta\cdot\hat{n}_t(x)}\delta(x - x(t)) \,.$$

Here $\hat{n}_t(x)$ is the discrete lattice translation defined in (24.3). Two kinds of orbits periodic in the elementary cell contribute. A periodic orbit is called *standing* if it is also periodic orbit of the infinite state space dynamics, $\hat{f}^{T_p}(x) = x$, and it is called *running* if it corresponds to a lattice translation in the dynamics on the infinite state space, $\hat{f}^{T_p}(x) = x + \hat{n}_p$. We recognize the shortest repeating segment of a running orbit as our old 'relative periodic orbit' friend from chapter 11. In the theory of area–preserving maps such as the standard map of example 8.7 these orbits are called *accelerator modes*, as the diffusion takes place along the momentum rather than the position coordinate. The traveled distance $\hat{n}_p = \hat{n}_{T_p}(x_0)$ is independent of the starting point x_0, as can be easily seen by continuing the path periodically in $\hat{\mathcal{M}}$.

The final result is the spectral determinant (22.5)

$$\det\left(s(\beta) - \mathcal{A}\right) = \prod_p \exp\left(-\sum_{r=1}^{\infty}\frac{1}{r}\frac{e^{(\beta\cdot\hat{n}_p - sT_p)r}}{\left|\det\left(\mathbf{1} - M_p^r\right)\right|}\right) , \tag{24.7}$$

or the corresponding dynamical zeta function (22.11)

$$1/\zeta(\beta, s) = \prod_p \left(1 - \frac{e^{(\beta\cdot\hat{n}_p - sT_p)}}{|\Lambda_p|}\right) . \tag{24.8}$$

The dynamical zeta function cycle averaging formula (23.24) for the diffusion constant (20.40), zero mean drift $\langle \hat{x}_i \rangle = 0$, is given by

$$D = \frac{1}{2d} \frac{\langle \hat{x}^2 \rangle_\zeta}{\langle T \rangle_\zeta} = \frac{1}{2d} \frac{1}{\langle T \rangle_\zeta} \sum{}' \frac{(-1)^{k+1} (\hat{n}_{p_1} + \cdots + \hat{n}_{p_k})^2}{|\Lambda_{p_1} \cdots \Lambda_{p_k}|} \,. \tag{24.9}$$

where the sum is over all distinct non-repeating combination of prime cycles. The derivation is standard, still the formula is strange. Diffusion is unbounded motion across an infinite lattice; nevertheless, the reduction to the elementary cell enables us to compute relevant quantities in the usual way, in terms of periodic orbits.

A sleepy reader might protest that $x(T_p) - x(0)$ is manifestly equal to zero for a periodic orbit. That is correct; $\hat{n}_p$ in the above formula refers to a displacement $\hat{x}(T_p)$ on the *infinite* periodic lattice, while p refers to closed orbit of the dynamics $f^t(x)$ reduced to the elementary cell, with x_p a periodic point in the closed prime cycle p.

Even so, this is not an obvious formula. Globally periodic orbits have $\hat{x}_p^2 = 0$, and contribute only to the time normalization $\langle T \rangle_\zeta$. The mean square displacement $\langle \hat{x}^2 \rangle_\zeta$ gets contributions only from the periodic runaway trajectories; they are closed in the elementary cell, but on the periodic lattice each one grows like $\hat{x}(t)^2 = (\hat{n}_p / T_p)^2 t^2 = v_p^2 t^2$. So the orbits that contribute to the trace formulas and spectral determinants exhibit either ballistic transport or no transport at all: diffusion arises as a balance between the two kinds of motion, weighted by the $1/|\Lambda_p|$ measure. If the system is not hyperbolic such weights may be abnormally large, with $1/|\Lambda_p| \approx 1/{T_p}^\alpha$ rather than $1/|\Lambda_p| \approx e^{-T_p \lambda}$, where λ is the Lyapunov exponent, and they may lead to anomalous diffusion - accelerated or slowed down depending on whether the probabilities of the running or the standing orbits are enhanced.

section 24.3

We illustrate the main idea, tracking of a globally diffusing orbit by the associated confined orbit restricted to the elementary cell, with a class of simple 1-dimensional dynamical systems where all transport coefficients can be evaluated analytically. For another example of deterministic diffusion in a Hamiltonian system, consult appendix A24.

appendix A24

24.2 Diffusion induced by chains of 1-dimensional maps

In a typical deterministic diffusive process, trajectories originating from a given scatterer reach a finite set of neighboring scatterers in one bounce, and then the process is repeated. As was shown in chapter 14, the essential part of this process is the stretching along the unstable directions of the flow, and in the crudest approximation the dynamics can be modeled by 1-dimensional expanding maps. This observation motivates introduction of a class of particularly simple 1-dimensional systems.

example 24.1
p. 465

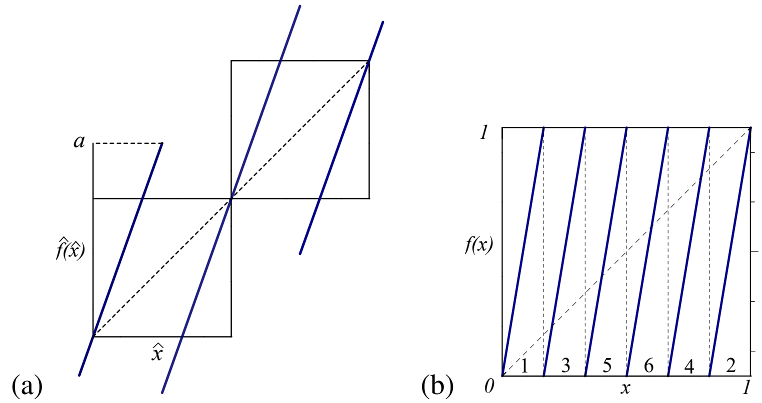

Figure 24.4: (a) $\hat{f}(\hat{x})$, the full space sawtooth map (24.21), $\Lambda > 2$. (b) $f(x)$, the sawtooth map restricted to the unit circle (24.24), $\Lambda = 6$.

As noted in sect. 24.1.1, the elementary cell cycles correspond to either standing or running orbits for the map on the full line: we shall refer to $\hat{n}_p \in \mathbb{Z}$ as the *jumping number* of the p cycle, and take as the cycle weight

$$t_p = z^{n_p} e^{\beta \hat{n}_p} / |\Lambda_p| \,. \tag{24.10}$$

The diffusion constant formula (24.9) for 1-dimensional maps is

$$D = \frac{1}{2} \frac{\langle \hat{n}^2 \rangle_\zeta}{\langle n \rangle_\zeta} \,, \tag{24.11}$$

where the "mean cycle time" is given by (23.25)

$$\langle n \rangle_\zeta = z \frac{\partial}{\partial z} \frac{1}{\zeta(0,z)} \bigg|_{z=1} = -\sum{}' (-1)^k \frac{n_{p_1} + \cdots + n_{p_k}}{|\Lambda_{p_1} \cdots \Lambda_{p_k}|} \,, \tag{24.12}$$

and the "mean cycle displacement squared" by (23.27)

$$\langle \hat{n}^2 \rangle_\zeta = \frac{\partial^2}{\partial \beta^2} \frac{1}{\zeta(\beta,1)} \bigg|_{\beta=0} = -\sum{}' (-1)^k \frac{(\hat{n}_{p_1} + \cdots + \hat{n}_{p_k})^2}{|\Lambda_{p_1} \cdots \Lambda_{p_k}|} \,, \tag{24.13}$$

the primed sum indicating all distinct non-repeating combinations of prime cycles. The evaluation of these formulas for the simple system of example 24.1 will require nothing more than pencil and paper.

example 24.2
p. 465

24.2.1 Higher order transport coefficients

The same approach yields higher order transport coefficients

$$\mathcal{B}_k = \frac{1}{k!} \frac{d^k}{d\beta^k} s(\beta) \bigg|_{\beta=0} \,, \qquad \mathcal{B}_2 = D \,, \tag{24.14}$$

known for $k > 2$ as the Burnett coefficients. The behavior of the higher order coefficients yields information on the relaxation to the asymptotic distribution function

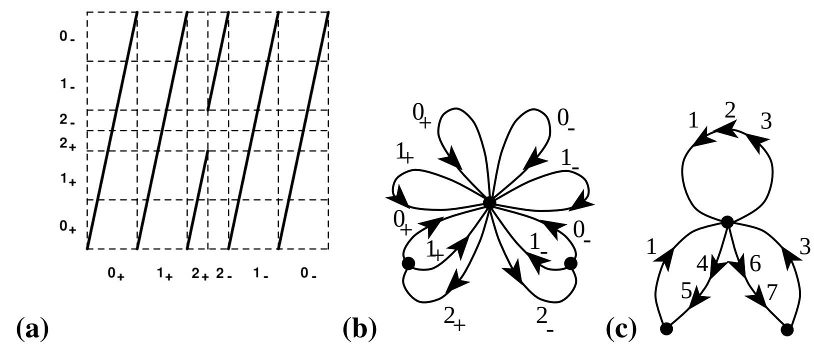

Figure 24.5: (a) A partition of the unit interval into six intervals, example 24.4, labeled by the jumping number $\hat{n}(x)$ $I = \{0_+, 1_+, 2_+, 2_-, 1_-, 0_-\}$. The partition is Markov, as the critical point is mapped onto the right border of $\mathcal{M}_{1_+}$. (b) The transition graph for this partition. (c) The transition graph in the compact Vadim Moroz notation of (24.32).

generated by the diffusive process. Here $\hat{x}_t$ is the relevant dynamical variable and $\mathcal{B}_k$'s are related to moments $\langle \hat{x}_t^k \rangle$ of arbitrary order.

Were the diffusive process purely Gaussian

$$e^{ts(\beta)} = \frac{1}{\sqrt{4\pi Dt}} \int_{-\infty}^{+\infty} d\hat{x}\, e^{\beta \hat{x}} e^{-\hat{x}^2/(4Dt)} = e^{\beta^2 Dt} \tag{24.15}$$

the only $\mathcal{B}_k$ coefficient different from zero would be $\mathcal{B}_2 = D$. Hence, nonvanishing higher order coefficients signal deviations of deterministic diffusion from a Gaussian stochastic process.

example 24.3
p. 466

We see that deterministic diffusion is not a Gaussian stochastic process. Higher order even coefficients may be calculated along the same lines.

24.2.2 Finite Markov partitions

For piecewise-linear maps exact results may be obtained whenever the critical points are mapped in finite numbers of iterations onto partition boundary points, or onto unstable periodic orbits. We will work out here an example for which this occurs in two iterations, leaving other cases as exercises. The key idea is to construct a *Markov partition* (14.2), with intervals mapped *onto* unions of intervals.

example 24.4
p. 466

It is by now clear how to build an infinite hierarchy of finite Markov partitions: tune the slope in such a way that the critical value $f(1/2)$ is mapped into the fixed point at the origin, $f^n(1/2) = 0$, in a finite number of iterations n. By taking higher and higher values of n one constructs a dense set of Markov parameter values, organized into a hierarchy that resembles the way in which rationals are densely embedded in the unit interval. For example, each of the 6 primary intervals can be subdivided into 6 intervals obtained by the 2-nd iterate of the map, and for the critical point mapping into any of those in 2 steps the grammar (and the corresponding cycle expansion) is finite. So, if we can prove continuity of $D = D(\Lambda)$, we can apply the periodic orbit theory to the sawtooth map (24.21) for a random "generic" value of the parameter Λ, for example $\Lambda = 4.5$. The idea is to bracket this value of Λ by a sequence of nearby Markov values, compute the exact diffusion constant for each such Markov partition, and study their convergence toward the value of D for $\Lambda = 4.5$. Some details of how this is accomplished are given in appendix A14.3 for a related problem, the pruned Bernoulli shift. Judging how difficult such problem is already for a tent map (see sect. 18.5), this is not likely to take only a week of work.

Expressions like (24.28) may lead to an expectation that the diffusion coefficient (and thus transport properties) are smooth functions of parameters controlling the chaoticity of the system. For example, one might expect that the diffusion coefficient increases smoothly and monotonically as the slope Λ of the map (24.21) is increased, or, perhaps more physically, that the diffusion coefficient is a smooth function of the Lyapunov exponent λ. This turns out not to be true: D as a function of Λ is a fractal, nowhere differentiable curve illustrated in figure 24.6. The dependence of D on the map parameter Λ is rather unexpected - even though for larger Λ more points are mapped outside the unit cell in one iteration, the diffusion constant does not necessarily grow.

This is a consequence of the lack of structural stability, even of purely hyperbolic systems such as the Lozi map and the 1-dimensional diffusion map (24.21). The trouble arises due to non-smooth dependence of the topological entropy on system parameters - any parameter change, no mater how small, leads to creation and destruction of infinitely many periodic orbits. As far as diffusion is concerned this means that even though local expansion rate is a smooth function of Λ, the number of ways in which the trajectory can re-enter the initial cell is an irregular function of Λ.

The lesson is that lack of structural stability implies lack of spectral stability, and no global observable is expected to depend smoothly on the system parameters. If you want to master the material, working through one of the deterministic diffusion projects on ChaosBook.org/pages is strongly recommended.

24.3 Marginal stability and anomalous diffusion

What effect does the intermittency of chapter 29 have on transport properties? A marginal fixed point affects the balance between the running and standing orbits, thus generating a mechanism that may result in anomalous diffusion.

example 24.5
p. 468

D vanishes by the implicit function theorem, $z''(\beta)|_{\beta=1} = 0$ when $\alpha \leq 1$. The physical interpretation is that a typical orbit will stick for long times near the $\overline{0}$

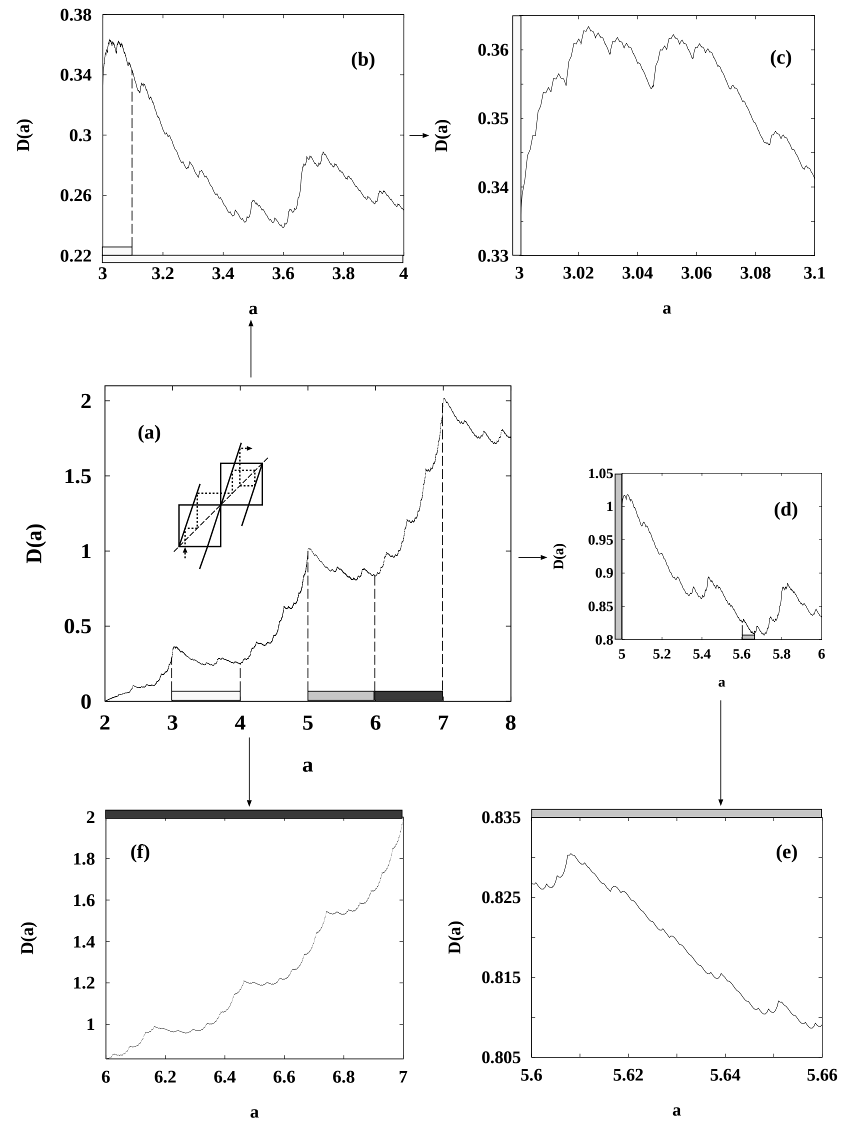

Figure 24.6: The dependence of D on the map parameter a is continuous, but not monotone. Here a stands for the slope Λ in (24.21). (From R. Klages thesis [29].)

marginal fixed point, and the 'trapping time' will be larger for higher values of the intermittency parameter s (recall $\alpha = 1/s$). In that case one needs to look more closely at the behavior of traces of high powers of the transfer operator.

The evaluation of transport coefficient requires one more derivative with respect to expectation values of state space observables (see sect. 24.1): if we use the diffusion dynamical zeta function (24.8), we may write the diffusion coefficient as an inverse Laplace transform, in such a way that the distinction between maps and flows has vanished. In the case of 1-dimensional diffusion we thus have

$$D = \lim_{t\to\infty} \frac{d^2}{d\beta^2} \frac{1}{2\pi i} \int_{a-i\infty}^{a+i\infty} ds\, e^{st} \frac{\zeta'(\beta,s)}{\zeta(\beta,s)}\bigg|_{\beta=0} \tag{24.16}$$

where the ζ' refers to the derivative with respect to s.

The evaluation of inverse Laplace transforms for high values of the argument is most conveniently performed using Tauberian theorems. We shall take

$$\omega(\lambda) = \int_0^\infty dx\, e^{-\lambda x} u(x)\,,$$

with $u(x)$ monotone as $x \to \infty$; then, as $\lambda \mapsto 0$ and $x \mapsto \infty$ respectively (and $\rho \in (0, \infty)$,

$$\omega(\lambda) \sim \frac{1}{\lambda^\rho} L\left(\frac{1}{\lambda}\right)$$

if and only if

$$u(x) \sim \frac{1}{\Gamma(\rho)} x^{\rho-1} L(x)\,,$$

where L denotes any slowly varying function with $\lim_{t\to\infty} L(ty)/L(t) = 1$. Now

$$\frac{1/\zeta_0{}'(e^{-s},\beta)}{1/\zeta_0(e^{-s},\beta)} = \frac{\left(\frac{4}{\Lambda} + \frac{\Lambda-4}{\Lambda\zeta(1+\alpha)}\left(J(e^{-s},\alpha+1) + J(e^{-s},\alpha)\right)\right)\cosh\beta}{1 - \frac{4}{\Lambda}e^{-s}\cosh\beta - \frac{\Lambda-4}{\Lambda\zeta(1+\alpha)}e^{-s}(e^{-s},\alpha+1)\cosh\beta J}\,.$$

Taking the second derivative with respect to β we obtain

$$\frac{d^2}{d\beta^2}\left(1/\zeta_0{}'(e^{-s},\beta)/\zeta^{-1}(e^{-s},\beta)\right)_{\beta=0}$$

$$= \frac{\frac{4}{\Lambda} + \frac{\Lambda-4}{\Lambda\zeta(1+\alpha)}\left(J(e^{-s},\alpha+1) + J(e^{-s},\alpha)\right)}{\left(1 - \frac{4}{\Lambda}e^{-s} - \frac{\Lambda-4}{\Lambda\zeta(1+\alpha)}e^{-s}J(e^{-s},\alpha+1)\right)^2} = g_\alpha(s)\,. \tag{24.17}$$

The asymptotic behavior of the inverse Laplace transform (24.16) may then be evaluated via Tauberian theorems, once we use our estimate for the behavior of Jonquière functions near $z = 1$. The deviations from normal behavior correspond to an explicit dependence of D on time. Omitting prefactors (which can be calculated by the same procedure) we have

$$g_\alpha(s) \sim \begin{cases} s^{-2} & \text{for } \alpha > 1 \\ s^{-(\alpha+1)} & \text{for } \alpha \in (0,1) \\ 1/(s^2 \ln s) & \text{for } \alpha = 1 \,. \end{cases}$$

The anomalous diffusion exponents follow:

exercise 24.6

$$\langle (x - x_0)^2 \rangle_t \sim \begin{cases} t^\alpha & \text{for } \alpha \in (0,1) \\ t/\ln t & \text{for } \alpha = 1 \\ t & \text{for } \alpha > 1 \,. \end{cases} \tag{24.18}$$

Résumé

Perfection itself is imperfection.
— Vladimir Horowitz

With initial data accuracy $\delta x = |\delta \mathbf{x}(0)|$ and system size L, a trajectory is predictable only to the finite Lyapunov time $T_{\text{Lyap}} \approx \lambda^{-1} \ln |L/\delta x|$. Beyond that, chaos rules. We have discussed the implications in sect. 1.8: chaos is good news for prediction of long term observables such as transport in statistical mechanics.

The classical Boltzmann equation for evolution of 1-particle density is based on *stosszahlansatz*, neglect of particle correlations prior to, or after a 2-particle collision. It is a very good approximate description of dilute gas dynamics, but a difficult starting point for inclusion of systematic corrections. In the theory developed here, no correlations are neglected - they are all included in the cycle averaging formula such as the cycle expansion for the diffusion constant

$$D = \frac{1}{2d} \frac{1}{\langle T \rangle_\zeta} \sum{}' (-1)^{k+1} \frac{(\hat{n}_{p_1} + \cdots + \hat{n}_{p_k})^2}{|\Lambda_{p_1} \cdots \Lambda_{p_k}|} \,.$$

Such formulas are *exact*; the issue in their applications is what are the most effective schemes of estimating the infinite cycle sums required for their evaluation. Here there are no phenomenological macroscopic parameters; quantities such as transport coefficients are calculable to any desired accuracy from the microscopic dynamics.

For systems of a few degrees of freedom these results are on rigorous footing, but there are indications that they capture the essential dynamics of systems of many degrees of freedom as well.

Though superficially indistinguishable from the probabilistic random walk diffusion, deterministic diffusion is quite recognizable, at least in low dimensional settings, through fractal dependence of the diffusion constant on the system parameters (see sect. 1.8), and through non-Gaussion relaxation to equilibrium (non-vanishing Burnett coefficients).

section 1.8

That Smale's "structural stability" conjecture turned out to be wrong is not a bane of chaotic dynamics - it is actually a virtue, perhaps its most dramatic experimentally measurable prediction. As long as microscopic periodicity of the physical system, such as a face of a crystal, is exact, the prediction is counterintuitive for a physicist - transport coefficients are *not* smooth functions of system parameters, rather they are non-monotonic, *nowhere differentiable* functions.

Commentary

Remark 24.1. Lorentz gas. The "Lorentz gas" is one of the simplest hyperbolic Hamiltonian dynamical systems that exhibits chaos and deterministic diffusion. The original Lorentz gas [36] assumed a random distribution of heavy scatterers; a description of such gas requires statistical assumptions about the distribution of scatterers. A periodic Lorenz gas (configuration of scatterers invariant under a discrete group of translations of the plane), however, is amenable to pure deterministic description. Ergodic properties of periodic Lorenz gases were first studied by Sinai [39], and its diffusive properties have been extensively studied ever since [8–11, 19, 22, 37]. One distinguishes the *infinite horizon* diffusive behavior, which allows for infinite length flights, from the *finite horizon* case [10], where the particle always hits the next disk in finite time, and the diffusion is normal [7, 10], with $\overline{\hat{x}(t)^2}$ growing like t. Most of the periodic Lorentz gas literature, such as Bunimovich and Sinai [10], is focused on the symmetries under discrete translations of periodic tilings of the plane, usually defined by a parallelepipedal "primitive unit cell" (also called "fundamental domain" in literature; here that term will be reserved for the smallest tile that tiles the hexagon). However, for a triangular periodic Lorentz gas the full symmetry group is the space group $p6mm$ (see Chapter 11 of ref. [13] for a discussion of the geometry of space groups), and the natural tiling is in terms of the hexagon centered on the scattering disk ("Wigner-Seitz cell", "Voronoi cell"). For a recent review see Dettmann [16].

Remark 24.2. Who's dunnit? Cycle expansions for the diffusion constant of a particle moving in a periodic array have been introduced by Artuso [1] (exact dynamical zeta function for 1-dimensional chains of maps (24.9)), by Vance [40] (who applied the Artuso [1] formula to the Lorentz gas) and by Cvitanović, Eckmann and Gaspard [14] (the dynamical zeta function cycle expansion (24.9) applied to the Lorentz gas). Attempts to evaluate the Lorentz gas dynamical zeta function cycle expansion were carried out by Schreiber [15] and Zhang [41].

Remark 24.3. Lack of structural stability for D. Expressions like (24.28) may lead to an expectation that the diffusion coefficient (and thus transport properties) are smooth functions of the chaoticity of the system (parameterized, for example, by the Lyapunov exponent $\lambda = \ln \Lambda$). This turns out not to be true: D as a function of Λ is a fractal, nowhere differentiable curve shown in figure 24.6. The dependence of D on the map parameter Λ is rather unexpected - even though for larger Λ more points are mapped outside the unit cell in one iteration, the diffusion constant does not necessarily grow. We refer the reader to refs. [23, 38] for early work on the deterministic diffusion induced by 1-dimensional maps. The sawtooth map (24.21) was introduced by Grossmann and Fujisaka [26] who derived the integer slope formulas (24.28) for the diffusion constant. The sawtooth map is also discussed in ref. [21]. The fractal dependence of diffusion constant on the map parameter is discussed in refs. [29, 32, 33]. Keller, Howard and Klages [28] show that for piecewise $C2$ expanding interval maps the diffusion coefficient D is Lipschitz continuous under parameter variations, up to quadratic logarithmic corrections. R. Klages lecture notes [31] a quick, first-year Ph.D. introduction to the concept of deterministic diffusion. For the current state of the art of fractal transport coefficients consult the first part of Klage's monograph [30]. Sect. 1.8 discusses briefly the experimental implications; would be sweet if someone actually check these predictions in an experiment. No fractal-like behavior of the conductivity for the Lorentz gas has been detected so far [35]. Statistical mechanicians (see, for example, Gallavotti and Cohen [20]) tend to believe that such complicated behavior is not to be expected in systems with very many degrees of freedom, as the addition to a large integer dimension of a number smaller than 1 should be as unnoticeable as a microscopic perturbation of a macroscopic quantity.

Remark 24.4. Symmetry factorization in one dimension. In the $\beta = 0$ limit the dynamics (24.23) is symmetric under $x \to -x$, and the zeta functions factorize into products of zeta functions for the symmetric and antisymmetric subspaces, as described in example 25.9:

$$
\begin{aligned}
\frac{1}{\zeta(0,z)} &= \frac{1}{\zeta_s(0,z)}\frac{1}{\zeta_a(0,z)} \\
\frac{\partial}{\partial z}\frac{1}{\zeta} &= \frac{1}{\zeta_s}\frac{\partial}{\partial z}\frac{1}{\zeta_a} + \frac{1}{\zeta_a}\frac{\partial}{\partial z}\frac{1}{\zeta_s}\,.
\end{aligned} \tag{24.19}
$$

The leading (material flow conserving) eigenvalue $z = 1$ belongs to the symmetric subspace $1/\zeta_s(0,1) = 0$, so the derivatives (24.12) also depend only on the symmetric subspace:

$$
\begin{aligned}
\langle n \rangle_\zeta &= z\frac{\partial}{\partial z}\frac{1}{\zeta(0,z)}\bigg|_{z=1} \\
&= \frac{1}{\zeta_a(0,z)}\, z\frac{\partial}{\partial z}\,\frac{1}{\zeta_s(0,z)}\bigg|_{z=1}\,.
\end{aligned} \tag{24.20}
$$

Remark 24.5. Lorentz gas in the fundamental domain. The vector valued nature of the moment-generating function (24.4) in the case under consideration makes it difficult to perform a calculation of the diffusion constant within the fundamental domain. Yet we point out that, at least as regards scalar quantities, the full reduction to $\tilde{\mathcal{M}}$ leads to better estimates. A proper symbolic dynamics in the fundamental domain has been introduced in ref. [12].

In order to perform the full reduction for diffusion one should express the dynamical zeta function (24.8) in terms of the prime cycles of the fundamental domain $\tilde{\mathcal{M}}$ of the lattice (see figure 24.3) rather than those of the elementary (Wigner-Seitz) cell $\mathcal{M}$. This problem is complicated by the breaking of the rotational symmetry by the auxiliary vector β, or, in other words, the non-commutativity of translations and rotations: see ref. [14]. For a 'fundamental domain' in hyperbolic geometry, see for example these notes by K. Martin.

Remark 24.6. Anomalous diffusion. Anomalous diffusion for 1-dimensional intermittent maps was studied in the continuous time random walk approach in refs. [24, 25].

T_p	# cycles	$\zeta(0,0)$	λ	D
1	5	-0.2169759	1.39193	0.37795
2	10	-0.0248233	1.74541	0.23118
3	33	-0.0221962	1.72235	0.25257
4	108	-0.0002192	1.74450	0.24165
5	373	0.0023463	1.76079	0.24468
6	1378	0.0096330	1.75610	0.24068
numerical experiment			1.760	0.25

Table 24.1: The Lyapunov exponent λ and the diffusion constant D computed in the fundamental domain, $w = 0.3$ disk-disk separation, disks radius = 1. (From Zhang*et al.* [41])

The first approach within the framework of cycle expansions (based on truncated dynamical zeta functions) was developed by Artuso *et al.* [2, 4]. For more recent developments, consult refs. [3, 6] and Klages, Radons and Sokolov [34]. Our treatment follows methods introduced in ref. [15], applied there to investigate the behavior of a Lorentz gas with unbounded horizon.

Question 24.1. Henriette Roux wants to know

Q Do these Jonquière functions appear in physics?

A In statistical mechanics Jonquière function (24.35) appears in the theory of free Bose-Einstein gas, see refs. [17, 18].

exercise 29.1

References

[1] R. Artuso, "Diffusive dynamics and periodic orbits of dynamic systems", Phys. Lett. A **160**, 528–530 (1991).

[2] R. Artuso, "Recycling deterministic diffusion", Physica D **76**, 1–7 (1994).

[3] R. Artuso and R. Burioni, "Anomalous diffusion: Deterministic and stochastic perspectives", in *Large Deviations in Physics: The Legacy of the Law of Large Numbers*, edited by A. Vulpiani, F. Cecconi, M. Cencini, A. Puglisi, and D. Vergni (Springer, Berlin, 2014), pp. 263–293.

[4] R. Artuso, G. Casati, and R. Lombardi, "Periodic orbit theory of anomalous diffusion", Phys. Rev. Lett. **71**, 62 (1993).

[5] R. Artuso, G. Casati, and R. Lombardi, "Periodic orbit theory of deterministic diffusion", Physica A **205**, 412–419 (1994).

[6] R. Artuso and G. Cristadoro, "Deterministic (anomalous) transport", in *Anomalous Transport: Foundations and Applications*, edited by R. Klages, G. Radons, and I. M. Sokolov (Wiley, New York, 2008).

[7] P. M. Bleher, "Statistical properties of two-dimensional periodic Lorentz gas with infinite horizon", J. Stat. Phys. **66**, 479–497 (1992).

[8] L. A. Bunimovich, "Decay of correlations in dynamical systems with chaotic behavior", Sov. Phys. JETP **62**, 842–852 (1985).

[9] L. A. Bunimovich and Y. G. Sinai, "Markov partitions for dispersed billiards", Commun. Math. Phys. **78**, Erratum, ibid. **107**, 357 (1986), 247–280 (1980).

[10] L. A. Bunimovich and Y. G. Sinai, "Statistical properties of Lorentz gas with periodic configuration of scatterers", Commun. Math. Phys. **78**, 479–497 (1981).

[11] L. A. Bunimovich, Y. G. Sinai, and N. I. Chernov, "Markov partitions for two-dimensional hyperbolic billiards", Russ. Math. Surv. **45**, 105–152 (1990).

[12] F. Christiansen, Analysis of Chaotic Dynamical Systems in Terms of Cycles, MA thesis (Univ. of Copenhagen, Copenhagen, 1989).

[13] F. A. Cotton, *Chemical Applications of Group Theory*, 3rd ed. (Wiley, New York, 2008).

[14] P. Cvitanović, J.-P. Eckmann, and P. Gaspard, "Transport properties of the Lorentz gas in terms of periodic orbits", Chaos Solit. Fract. **6**, 113–120 (1995).

[15] P. Cvitanović, P. Gaspard, and T. Schreiber, "Investigation of the Lorentz gas in terms of periodic orbits", Chaos **2**, 85–90 (1992).

[16] C. P. Dettmann, "Diffusion in the Lorentz gas", Commun. Theor. Phys **62**, 521–540 (2014).

[17] A. Erdélyi, W. Magnus, F. Oberhettinger, and F. G. Tricomi, *Higher Transcendental Functions*, Vol. 1, Bateman Manuscript Project (McGraw-Hill, 1953).

[18] B. Fornberg and K. S. Kölbig, "Complex zeros of the Jonquière or polylogarithm function", Math. Comp. **29**, 582–599 (1975).

[19] G. Gallavotti, "Lectures on the billiard", in *Dynamical Systems, Theory and Applications*, Vol. 38, edited by J. Moser, Lecture Notes in Physics (Springer, Berlin, 1975), pp. 236–295.

[20] G. Gallavotti and E. G. D. Cohen, "Dynamical ensembles in nonequilibrium statistical mechanics", Phys. Rev. Lett. **74**, 2694–2697 (1995).

[21] P. Gaspard and F. Baras, Dynamical chaos underlying diffusion in the Lorentz gas, in Microscopic simulations of complex hydrodynamic phenomena, edited by M. Mareschal and B. L. Holian (1992) Chap. Microscopic simulations of complex hydrodynamic phenomena, pp. 301–322.

[22] P. Gaspard and G. Nicolis, "Transport properties, Lyapunov exponents, and entropy per unit time", Phys. Rev. Lett. **65**, 1693–1696 (1990).

[23] T. Geisel and J. Nierwetberg, "Onset of diffusion and universal scaling in chaotic systems", Phys. Rev. Lett. **48**, 7 (1982).

[24] T. Geisel, J. Nierwetberg, and A. Zacherl, "Accelerated diffusion in Josephson junctions and related chaotic systems", Phys. Rev. Lett. **54**, 616 (1985).

[25] T. Geisel and S. Thomae, "Anomalous diffusion in intermittent chaotic systems", Phys. Rev. Lett. **52**, 1936 (1984).

[26] S. Grossmann and H. Fujisaka, "Diffusion in discrete nonlinear dynamical systems", Phys. Rev. A **26**, 1779–1782 (1982).

[27] S. Grossmann and S. Thomae, "Shape dependence of correlation times in chaos-induced diffusion", Phys. Lett. A **97**, 263–267 (1983).

[28] G. Keller, P. J. Howard, and R. Klages, "Continuity properties of transport coefficients in simple maps", Nonlinearity **21**, 1719–1743 (2008).

[29] R. Klages, *Deterministic Diffusion in One-dimensional Chaotic Dynamical Systems* (Wissenschaft and Technik-Verlag, Berlin, 1996).

[30] R. Klages, *Microscopic Chaos, Fractals and Transport in Nonequilibrium Statistical Mechanics* (World Scientific, Singapore, 2007).

[31] R. Klages, From deterministic chaos to anomalous diffusion, 2008.

[32] R. Klages and J. R. Dorfman, "Simple maps with fractal diffusion coefficients", Phys. Rev. Lett. **74**, 387–390 (1995).

[33] R. Klages and J. R. Dorfman, "Dynamical crossover in deterministic diffusion", Phys. Rev. E **55**, R1247–R1250 (1997).

[34] R. Klages, G. Radons, and I. M. Sokolov, *Anomalous Transport: Foundations and Applications* (Wiley, New York, 2008).

[35] J. Lloyd, M. Niemeyer, L. Rondoni, and G. P. Morriss, "The nonequilibrium Lorentz gas", Chaos **5**, 536–551 (1995).

[36] H. A. Lorentz, "The motion of electrons in metallic bodies", K. Ned. Akad. van Wet. B **7**, 438–453 (1905).

[37] J. Machta and R. Zwanzig, "Diffusion in a periodic Lorentz gas", Phys. Rev. Lett. **50**, 1959–1962 (1983).

[38] M. Schell, S. Fraser, and R. Kapral, "Diffusive dynamics in systems with translational symmetry: A one–dimensional–map model", Phys. Rev. A **26**, 504–521 (1982).

[39] Y. G. Sinai, "Dynamical systems with elastic reflections", Russ. Math. Surv. **25**, 137–189 (1970).

[40] W. N. Vance, "Unstable periodic-orbits and transport-properties of nonequilibrium steady-states", Phys. Rev. Lett. **69**, 1356–1359 (1992).

[41] T. Zhang, P. Cvitanović, and D. I. Goldman, Diffuse globally, compute locally: a cyclist tale, In preparation, 2017.

24.4 Examples

Example 24.1. Chains of piecewise linear maps. We start by defining the map $\hat{f}$ on the unit interval as

$$\hat{f}(\hat{x}) = \begin{cases} \Lambda\hat{x} & \hat{x} \in [0, 1/2) \\ \Lambda\hat{x} + 1 - \Lambda & \hat{x} \in (1/2, 1] \end{cases}, \qquad \Lambda > 2\,, \tag{24.21}$$

and then extending the dynamics to the entire real line, by imposing the translation property

$$\hat{f}(\hat{x} + \hat{n}) = \hat{f}(\hat{x}) + \hat{n} \qquad \hat{n} \in \mathbb{Z}\,. \tag{24.22}$$

As the map is discontinuous at $\hat{x} = 1/2$, $\hat{f}(1/2)$ is undefined, and the $x = 1/2$ point has to be excluded from the Markov partition. The map is antisymmetric under the $\hat{x}$-coordinate flip

$$\hat{f}(\hat{x}) = -\hat{f}(-\hat{x})\,, \tag{24.23}$$

so the dynamics will exhibit no mean drift; all odd derivatives of the moment-generating function (20.10) with respect to β, evaluated at $\beta = 0$, will vanish.

The map (24.21) is sketched in figure 24.4 (a). Initial points sufficiently close to either of the fixed points in the initial unit interval remain in the elementary cell for one iteration; depending on the slope Λ, other points jump $\hat{n}$ cells, either to the right or to the left. Repetition of this process generates a random walk for almost every initial condition.

The translational symmetry (24.22) relates the unbounded dynamics on the real line to dynamics restricted to the elementary cell - in the example at hand, the unit interval curled up into a circle. Associated to $\hat{f}(\hat{x})$ we thus also consider the circle map

$$f(x) = \hat{f}(\hat{x}) - \left[\hat{f}(\hat{x})\right], \qquad x = \hat{x} - [\hat{x}] \in [0, 1] \tag{24.24}$$

figure 24.4 (b), where $[\cdots]$ stands for the integer part (24.3). For the piecewise linear map of figure 24.4 we can evaluate the dynamical zeta function in closed form. Each branch has the same value of the slope, and the map can be parameterized by a single parameter, for example its critical value $a = \hat{f}(1/2)$, the absolute maximum on the interval $[0, 1]$ related to the slope of the map by $a = \Lambda/2$. The larger Λ is, the stronger is the stretching action of the map.

click to return: p. 455

Example 24.2. Unrestricted symbolic dynamics. Whenever Λ is an integer number, the symbolic dynamics is exceedingly simple. For example, for the case $\Lambda = 6$ illustrated in figure 24.4 (b), the elementary cell map consists of 6 full branches, with uniform stretching factor $\Lambda = 6$. The branches have different jumping numbers: for branches 1 and 2 we have $\hat{n} = 0$, for branch 3 we have $\hat{n} = +1$, for branch 4 $\hat{n} = -1$, and finally for branches 5 and 6 we have respectively $\hat{n} = +2$ and $\hat{n} = -2$. The same structure reappears whenever Λ is an even integer $\Lambda = 2a$: all branches are mapped onto the whole unit interval and we have two $\hat{n} = 0$ branches, one branch for which $\hat{n} = +1$ and one for which $\hat{n} = -1$, and so on, up to the maximal jump $|\hat{n}| = a - 1$. The symbolic dynamics is thus full, unrestricted shift in $2a$ symbols $\{0_+, 1_+, \ldots, (a-1)_+, (a-1)_-, \ldots, 1_-, 0_-\}$, where the symbol indicates both the length and the direction of the corresponding jump.

For the piecewise linear maps with uniform stretching the weight associated with a given symbol sequence is a product of weights for individual steps, $t_{sq} = t_s t_q$. For the map of figure 24.4 there are 6 distinct weights (24.10):

$$
\begin{aligned}
t_1 &= t_2 = z/\Lambda \\
t_3 &= e^{\beta} z/\Lambda\,, \quad t_4 = e^{-\beta} z/\Lambda\,, \quad t_5 = e^{2\beta} z/\Lambda\,, \quad t_6 = e^{-2\beta} z/\Lambda\,.
\end{aligned}
$$

The piecewise linearity and the simple symbolic dynamics lead to the full cancelation of all curvature corrections in (23.8). The *exact* dynamical zeta function (18.13) is given by the fixed point contributions:

$$
\begin{aligned}
1/\zeta(\beta, z) &= 1 - t_{0_+} - t_{0_-} - \cdots - t_{(a-1)_+} - t_{(a-1)_-} \\
&= 1 - \frac{z}{a}\left(1 + \sum_{j=1}^{a-1} \cosh(\beta j)\right). \qquad (24.25)
\end{aligned}
$$

The leading (and only) eigenvalue of the evolution operator (24.6) is

$$
s(\beta) = \log\left\{\frac{1}{a}\left(1 + \sum_{j=1}^{a-1} \cosh(\beta j)\right)\right\}, \qquad \Lambda = 2a,\ a \text{ integer}. \qquad (24.26)
$$

The flow conservation (23.17) sum rule is manifestly satisfied, so $s(0) = 0$. The first derivative $s(0)'$ vanishes as well by the left/right symmetry of the dynamics, implying vanishing mean drift $\langle \hat{x} \rangle = 0$. The second derivative $s(\beta)''$ yields the diffusion constant (24.11):

$$
\langle n \rangle_\zeta = 2a\frac{1}{\Lambda} = 1\,, \qquad \langle \hat{x}^2 \rangle_\zeta = 2\frac{0^2}{\Lambda} + 2\frac{1^2}{\Lambda} + 2\frac{2^2}{\Lambda} + \cdots + 2\frac{(a-1)^2}{\Lambda} \qquad (24.27)
$$

Using the identity $\sum_{k=1}^{n} k^2 = n(n+1)(2n+1)/6$ we obtain

$$
D = \frac{1}{24}(\Lambda - 1)(\Lambda - 2)\,, \qquad \Lambda \text{ even integer}. \qquad (24.28)
$$

Similar calculation for odd integer $\Lambda = 2k - 1$ yields

exercise 24.1

$$
D = \frac{1}{24}(\Lambda^2 - 1)\,, \qquad \Lambda \text{ odd integer}. \qquad (24.29)
$$

click to return: p. 456

Example 24.3. $\mathcal{B}_4$ Burnett coefficient. For the map under consideration the first Burnett coefficient coefficient $\mathcal{B}_4$ (or kurtosis (20.20)) is easily evaluated. For example, using (24.26) in the case of even integer slope $\Lambda = 2a$ we obtain

exercise 24.2

$$
\mathcal{B}_4 = -\frac{1}{4! \cdot 60}(a-1)(2a-1)(4a^2 - 9a + 7)\,. \qquad (24.30)
$$

click to return: p. 457

Example 24.4. A finite Markov partition. As an example we determine a value of the parameter $4 \leq \Lambda \leq 6$ for which $f(f(1/2)) = 0$. As in the integer Λ case, we partition the unit interval into six intervals, labeled by the jumping number $\hat{n}(x) \in \{\mathcal{M}_{0_+}, \mathcal{M}_{1_+}, \mathcal{M}_{2_+}, \mathcal{M}_{2_-}, \mathcal{M}_{1_-}, \mathcal{M}_{0_-}\}$, ordered by their placement along the unit interval, figure 24.5 (a).

In general the critical value $a = \hat{f}(1/2)$ will not correspond to an interval border, but now we choose a such that the critical point is mapped onto the right border of $\mathcal{M}_{1_+}$. Equating $f(1/2)$ with the right border of $\mathcal{M}_{1_+}$, $x = 1/\Lambda$, we obtain a quadratic equation with the expanding solution $\Lambda = 2(\sqrt{2}+1)$. For this parameter value $f(\mathcal{M}_{2_+}) = \mathcal{M}_{0_+} \bigcup \mathcal{M}_{1_+}$, $f(\mathcal{M}_{2_-}) = \mathcal{M}_{0_-} \bigcup \mathcal{M}_{1_-}$, while the remaining intervals map onto the whole unit interval $\mathcal{M}$. The transition matrix (17.1) is given by

$$\phi' = T\phi = \begin{bmatrix} 1 & 1 & 1 & 0 & 1 & 1 \\ 1 & 1 & 1 & 0 & 1 & 1 \\ 1 & 1 & 0 & 0 & 1 & 1 \\ 1 & 1 & 0 & 0 & 1 & 1 \\ 1 & 1 & 0 & 1 & 1 & 1 \\ 1 & 1 & 0 & 1 & 1 & 1 \end{bmatrix} \begin{bmatrix} \phi_{0_+} \\ \phi_{1_+} \\ \phi_{2_+} \\ \phi_{2_-} \\ \phi_{1_-} \\ \phi_{0_-} \end{bmatrix}. \tag{24.31}$$

One could diagonalize (24.31) on a computer, but, as we saw in chapter 17, the transition graph of figure 24.5 (b) corresponding to map figure 24.5 (a) offers more insight into the dynamics. Figure 24.5 (b) can be redrawn more compactly as transition graph figure 24.5 (c) by replacing parallel lines in a graph by their sum

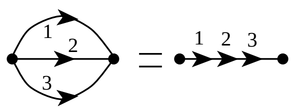

$$= t_1 + t_2 + t_3 \,. \tag{24.32}$$

The dynamics is unrestricted in the alphabet

$$\mathcal{A} = \{0_+,\ 1_+,\ 2_+0_+,\ 2_+1_+,\ 2_-1_-,\ 2_-0_-,\ 1_-,\ 0_-\}\,.$$

Applying the loop expansion (18.13) of sect. 18.3, we are led to the dynamical zeta function

$$\begin{aligned} 1/\zeta(\beta, z) &= 1 - t_{0_+} - t_{1_+} - t_{2_+0_+} - t_{2_+1_+} - t_{2_-1_-} - t_{2_-0_-} - t_{1_-} - t_{0_-} \\ &= 1 - \frac{2z}{\Lambda}(1+\cosh(\beta)) - \frac{2z^2}{\Lambda^2}(\cosh(2\beta)+\cosh(3\beta))\,. \end{aligned} \tag{24.33}$$

For grammar as simple as this one, the dynamical zeta function is the sum over fixed points of the unrestricted alphabet. As the first check of this expression for the dynamical zeta function we verify that

$$1/\zeta(0,1) = 1 - \frac{4}{\Lambda} - \frac{4}{\Lambda^2} = 0\,,$$

as required by the flow conservation (23.17). Conversely, we could have started by picking the desired Markov partition, writing down the corresponding dynamical zeta function, and then fixing Λ by the $1/\zeta(0,1) = 0$ condition. For more complicated transition graphs this approach, together with the factorization (24.19), is helpful in reducing the order of the polynomial condition that fixes Λ.

The diffusion constant follows from (24.11)

exercise 24.3

$$\begin{aligned} \langle n \rangle_\zeta &= 4\frac{1}{\Lambda} + 4\frac{2}{\Lambda^2}\,, \quad \langle \hat{n}^2 \rangle_\zeta = 2\frac{1^2}{\Lambda} + 2\frac{2^2}{\Lambda^2} + 2\frac{3^2}{\Lambda^2} \\ D &= \frac{15 + 2\sqrt{2}}{16 + 8\sqrt{2}}\,. \end{aligned} \tag{24.34}$$

click to return: p. 457

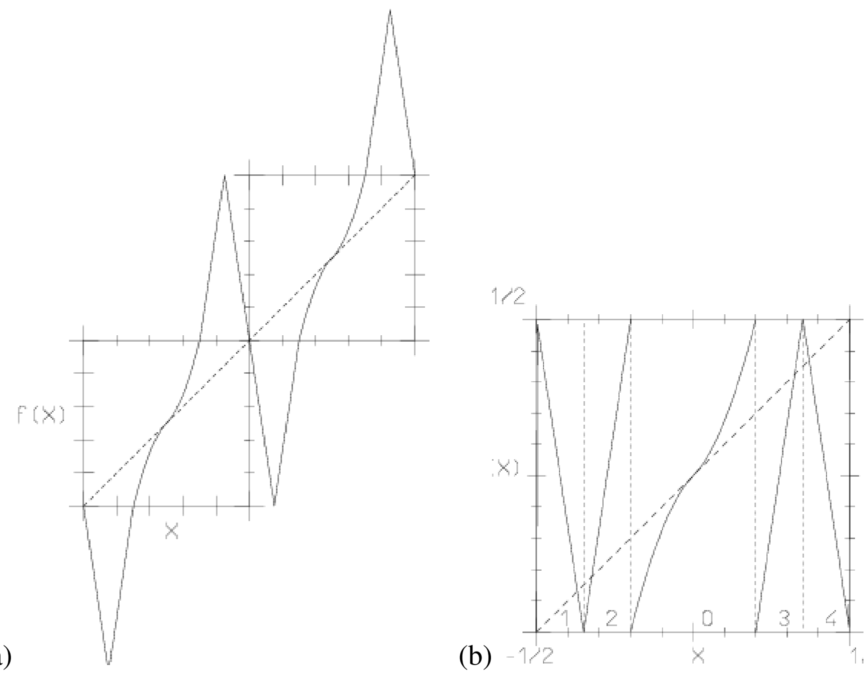

Figure 24.7: (a) A map with marginal fixed point. (b) The map restricted to the unit circle.

Example 24.5. Anomalous diffusion. Consider a 1-dimensional map of the real line on itself shown in figure 24.7 (a), with the same properties as in sect. 24.2, except for a marginal fixed point at $x = 0$. The corresponding circle map is given in figure 24.7 (b).

As in sect. 29.2.1, a branch with support in $\mathcal{M}_i$, $i = 1, 2, 3, 4$ has constant slope Λ_i, while $f|_{\mathcal{M}_0}$ is of intermittent form. To keep you nimble, this time we take a slightly different choice of slopes. The toy example of sect. 29.2.1 was cooked up so that the $1/s$ branch cut in dynamical zeta function was the whole answer. Here we shall take a slightly different route, and pick piecewise constant slopes such that the dynamical zeta function for intermittent system can be expressed in terms of the Jonquière function

question 24.1

$$J(z, s) = \sum_{k=1}^{\infty} z^k / k^s . \tag{24.35}$$

Once the $\overline{0}$ fixed point is pruned away, the symbolic dynamics is given by the infinite alphabet $\{1, 2, 3, 4, 0^i 1, 0^j 2, 0^k 3, 0^l 4\}$, $i, j, k, l = 1, 2, \ldots$ (compare with table 29.1). The partitioning of the subinterval $\mathcal{M}_0$ is induced by $\mathcal{M}_{0^k(right)} = \hat{f}^{-k}_{(right)}(\mathcal{M}_3 \cup \mathcal{M}_4)$ (where $\hat{f}^{-1}_{(right)}$ denotes the inverse of the right branch of $\hat{f}|_{\mathcal{M}_0}$) and the same reasoning applies to the leftmost branch. These are regions over which the slope of $\hat{f}|_{\mathcal{M}_0}$ is constant. Thus we have the following stabilities and jumping numbers associated to letters:

$$\begin{array}{rll} 0^k 3,\ 0^k 4 & \Lambda_p = \frac{k^{1+\alpha}}{q/2} & \hat{n}_p = 1 \\ 0^l 1,\ 0^l 2 & \Lambda_p = \frac{l^{1+\alpha}}{q/2} & \hat{n}_p = -1 \\ 3,\ 4 & \Lambda_p = \pm\Lambda & \hat{n}_p = 1 \\ 2,\ 1 & \Lambda_p = \pm\Lambda & \hat{n}_p = -1\,, \end{array} \tag{24.36}$$

where $\alpha = 1/s$ is determined by the intermittency exponent (29.1), while q is to be determined by the flow conservation (23.17) for $\hat{f}$:

$$\frac{4}{\Lambda} + 2q\zeta(\alpha + 1) = 1$$

(where ζ is the Riemann zeta function), so that $q = (\Lambda - 4)/(2\Lambda\zeta(\alpha + 1))$. The dynamical zeta function picks up contributions just by the alphabet's letters, as we have imposed piecewise linearity, and can be expressed in terms of a Jonquière function (24.35):

$$1/\zeta_0(z,\beta) \;=\; 1 - \frac{4}{\Lambda} z \cosh\beta - \frac{\Lambda - 4}{\Lambda\zeta(1+\alpha)} z \cosh\beta \cdot J(z, \alpha + 1)\,. \tag{24.37}$$

Its first zero $z(\beta)$ is determined by

$$\frac{4}{\Lambda} z + \frac{\Lambda - 4}{\Lambda\zeta(1+\alpha)} z \cdot J(z, \alpha + 1) \;=\; \frac{1}{\cosh\beta}\,.$$

click to return: p. 458

Exercises

24.1. **Diffusion for odd integer Λ.** Show that when the slope $\Lambda = 2k-1$ in (24.21) is an odd integer, the diffusion constant is given by $D = (\Lambda^2 - 1)/24$, as stated in (24.29).

24.2. **Fourth-order transport coefficient.** Verify (24.30). You will need the identity

$$\sum_{k=1}^{n} k^4 = \frac{1}{30} n(n+1)(2n+1)(3n^2+3n-1)\,.$$

24.3. **Finite Markov partitions.** Verify (24.34).

24.4. **Maps with variable peak shape:** Consider the following piecewise linear map

$$f_\delta(x) = \begin{cases} \frac{3x}{1-\delta} & x \in \mathcal{M}_1 \\ \frac{3}{2} - \left(\frac{2}{\delta}\left|\frac{4-\delta}{12} - x\right|\right) & x \in \mathcal{M}_2 \\ 1 - \frac{3}{1-\delta}\left(x - \frac{1}{6}(2+\delta)\right) & x \in \mathcal{M}_3 \end{cases}$$

where $\mathcal{M}_1 = \left[0, \frac{1}{3}(1-\delta)\right]$, $\mathcal{M}_2 = \left[\frac{1}{3}(1-\delta), \frac{1}{6}(2+\delta)\right]$, $\mathcal{M}_3 = \left[\frac{1}{6}(2+\delta), \frac{1}{2}\right]$, and the map in $[1/2, 1]$ is obtained by antisymmetry with respect to $x = 1/2$, $y = 1/2$. Write the corresponding dynamical zeta function relevant to diffusion and then show that

$$D = \frac{\delta(2+\delta)}{4(1-\delta)}$$

See refs. [5, 27] for further details.

24.5. **Two-symbol cycles for the Lorentz gas.** Write down all cycles labeled by two symbols, such as (0 6), (1 7), (1 5) and (0 5).

ChaosBook.org/projects offers several project-length deterministic diffusion exercises.

24.6. **Accelerated diffusion.** (medium difficulty) Consider a map h, such that $\hat{h} = \hat{f}$ of figure 24.7 (b), but now running branches are turned into standing branches and vice versa, so that $1, 2, 3, 4$ are standing while 0 leads to both positive and negative jumps. Build the corresponding dynamical zeta function and show that

$$\sigma^2(t) \sim \begin{cases} t & \text{for } \alpha > 2 \\ t\ln t & \text{for } \alpha = 2 \\ t^{3-\alpha} & \text{for } \alpha \in (1,2) \\ t^2/\ln t & \text{for } \alpha = 1 \\ t^2 & \text{for } \alpha \in (0,1) \end{cases}$$

24.7. **Recurrence times for Lorentz gas with infinite horizon.** Consider the Lorentz gas with unbounded horizon with a square lattice geometry, with disk radius R and unit lattice spacing. Label disks according to the (integer) coordinates of their center: the sequence of recurrence times $\{t_j\}$ is given by the set of collision times. Consider orbits that leave the disk sitting at the origin and hit a disk far away after a free flight (along the horizontal corridor). Initial conditions are characterized by coordinates (ϕ, α) (ϕ determines the initial position along the disk, while α gives the angle of the initial velocity with respect to the outward normal: the appropriate measure is then $d\phi\,\cos\alpha\,d\alpha$ ($\phi \in [0, 2\pi)$, $\alpha \in [-\pi/2, \pi/2]$. Find how $\phi(T)$ scales for large values of T: this is equivalent to investigating the scaling of portions of the state space that lead to a first collision with disk $(n, 1)$, for large values of n (as $n \mapsto \infty$ $n \simeq T$).

24.8. **Diffusion reduced to the fundamental domain.** Maps such as figure 24.4 are antisymmetric. Reduce such antisymmetric maps as in example 10.5, and write down the formula (24.11) for the diffusion constant D in terms of the fundamental domain cycles (relative periodic orbits) alone (P. Gaspard says it cannot be done [14]).